 ©2021 Kvantovaya Elektronika and IOP Publishing Limited

https://doi.org/10.1070/QEL17417

Time compression of frequency-modulated pulses in fibres with in-fibre refractive index gratings

A.S. Abramov, I.O. Zolotovskii, V.A. Kamynin, V.A. Lapin

Abstract. **The dynamics of frequency-modulated pulses in fibres with sequentially inscribed refractive-index gratings having a different period is considered. It is shown that the proposed structure of the fibre can be used to generate picosecond and subpicosecond pulses with peak powers on the order of 1 MW.**

Keywords: *frequency modulated pulse, refractive index gratings, time compression.*

1. Introduction

Since the advent of the laser, the most important branch of laser physics has been the development of ultrashort pulse generators, which provide a high peak radiation power. At present, such laser systems are in demand in many topical applications, including the processing and modification of materials, doping technologies, optical communications, medicine, nuclear and accelerator technologies, etc. [1–7].

One of the most common approaches used to obtain ultrashort pulses (USPs) is to generate pulses with a wide spectrum and linear frequency modulation (chirp) and then to compress them on an external compressor to compensate for the chirp. In practice, either a pair of diffraction gratings (prisms) or an anomalous-dispersion optical fibre is usually used as a compressor [8–10]. It was shown in [11–14] that the compression of frequency-modulated pulses (FMPs) of picosecond duration is especially effective in optical fibres with an exponential profile of the group velocity dispersion (GVD) distribution.

The corresponding mechanism of FMP compression was considered using the example of inhomogeneous fibres with a W-shaped refractive index (RI) distribution profile [15, 16]. This mechanism of temporal compression of pulses may be most promising when realising a single-mode regime of large-mode-area radiation propagation, provided that mode stability is preserved. Increasing the field area of a fibre mode is one of the main ways to increase power and reduce negative nonlinear distortions during radiation propagation. Such fibres include, for example, tapered fibres, which ensure the stability of a single-mode radiation propagation regime with a significant increase in the effective mode area [17–22].

In the last decade, another promising technique has been developed, which makes it possible to ensure the generation of large-mode-area single-mode wave packets (WPs). It consists in the mechanism of 'self-cleaning' of wave beams in multimode gradient fibres (first of all, in parabolic-index fibres) [23–31]. In this case, a significant technical obstacle arises for realising the regime of strong time compression of FMPs in gradient fibres: in contrast to fibres with a transverse W-shaped RI profile, the value of the group velocity dispersion in these fibres is usually determined only by the dispersion of the material. One of the solutions to this problem can be the 'inscription' of RI gratings with a smoothly increasing period along the entire length of the fibre. In this work, we propose a method for compressing FMPS in a fibre with sequentially placed RI gratings having different periods and, as a consequence, with a sharply decreasing GVD value. It should be noted that the technology of manufacturing periodic RI gratings has been quite well developed by now [32, 33]. For example, the specific features of the inscription of RI gratings in gradient multimode fibres are considered in detail in Refs [34–41].

2. Basic relations

The geometry of the considered waveguide structure with segments containing varying-period RI gratings is shown in Fig. 1. In the corresponding segments of the fibre, the distribution of the refractive index along the length is given by the relation [32–37]

$$n_i(z) = n_0[1 - m\cos(2\pi z/\Lambda_i(z))], \quad (1)$$

where n_0 is the average refractive index of the fibre in the absence of the grating, m is the modulation depth of the RI grating, and Λ_i is its period.

It is known that the contribution to the effective GVD made by the RI grating is much greater than the contribution

A.S. Abramov, I.O. Zolotovskii, V.A. Lapin Ulyanovsk State University, ul. L. Tolstogo 42, 432017 Ulyanovsk, Russia; e-mail: aleksei_abramov@mail.ru;
V.A. Kamynin Prokhorov General Physics Institute of the Russian Academy of Sciences, ul. Vavilova 38, 119991 Moscow, Russia

Received 6 August 2020; revision received 27 October 2020
Kvantovaya Elektronika **51** (2) 153–157 (2021)
Translated by I.A. Ulitkin

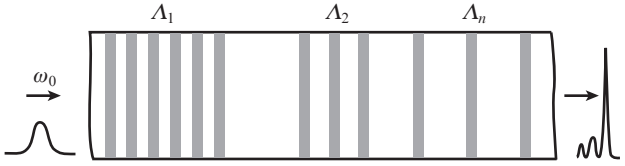

Figure 1. Geometry of the structure in question.

made by the material dispersion of the fibres. In this case, the expression for the second-order GVD takes the form [41–44]

$$\beta_2(z) = d_2 - \frac{\mathrm{sign}(\delta)\kappa^2}{V_g^2(\delta^2-\kappa^2)^{3/2}} \approx d_2 - \frac{\mathrm{sign}(\delta)\kappa^2}{V_g^2\delta^3}, \quad (2)$$

where

$$d_2 = \frac{1}{c}\left[\frac{\partial^2(\omega n_0(\omega))}{\partial\omega^2}\right]_{\omega=\omega_0}$$

is the second-order dispersion parameter, determined by the fibre material, and V_g is the group velocity of a wave packet in a fibre without an in-fibre grating. The parameter κ determines the coupling coefficient between the direct and reflected waves, takes into account the transverse changes in the RI, and in the case of a homogeneous grating can be written as $\kappa = 2\pi m/\lambda_0$, where λ_0 is the centre (carrier) pulse wavelength. The quantity determines the detuning of the carrier frequency ω_0 from the Bragg matching frequency ω_B:

$$\delta_i(z) = \frac{\omega_0 - \omega_{Bi}(z)}{V_g} = \frac{2\pi c}{V_g}\left(\frac{1}{\lambda_0} - \frac{1}{\lambda_{Bi}(z)}\right) = \frac{2\pi c}{V_g\lambda_0} - \frac{\pi}{\Lambda_i(z)}. \quad (3)$$

The sign of the parameter δ_i determines the sign of the second-order dispersion β_2 of the corresponding lattice. Group velocity dispersion takes negative values in the spectral region, where the carrier wavelength is less than the Bragg wavelength [42, 43]. Further analysis will be carried out under the condition of large detuning from Bragg matching: $|\delta| \gg \kappa$, that is, we will assume that the carrier frequency of the WP is far from the Bragg frequency (band gap). For the band gap, we obtain the relation $\Delta\lambda_{gap} = m\lambda_0/2n_0 \ll 1$ nm.

Note that, under conditions of large detuning from Bragg matching, the RI grating weakly affects the effective cubic (Kerr) nonlinearity, which in our case is determined exclusively by the material parameters of the fibre. In this case, the use of RI gratings as dispersing elements inevitably leads to a strong influence of higher-order dispersion effects. The third-order GVD is determined by the relation [41–44]

$$\beta_3(z) = d_3 + \frac{3\delta\kappa^2}{V_g^3\left(\delta^2-\kappa^2\right)^{5/2}} \approx \frac{3\mathrm{sign}(\delta)\kappa^2}{V_g^3\delta^4}, \quad (4)$$

where

$$d_3 = \frac{1}{c}\left[\frac{\partial^3(\omega n_0(\omega))}{\partial\omega^3}\right]_{\omega=\omega_0}.$$

Analysis shows that in a 'standard' single-mode fibre, the value of the parameter $\beta_3(z)$ is several orders of magnitude higher than the third-order material dispersion d_3 [42, 45]. This circumstance negatively affects the quality of the FMP compression and can lead to a strong distortion of the pulse shape, including its rapid destruction.

An increase in the period $\Lambda(z)$ of the inscribed RI gratings makes it possible to increase the detuning δ and, as a consequence, leads to a gradual decrease in the absolute value of the anomalous GVD. Thus, it can be seen from relations (2) and (4) that in the case of an increase in the period of a conditional grating, the rate of a decrease in the second- and third-order dispersion parameters occurs in proportion to δ^{-3} and δ^{-4}, respectively. Thus, a rapid increase in the parameter δ along the length of the fibre leads to an even more rapid decrease in the influence of dispersion parameters of higher orders (in the ratio $\beta_n{:}\delta^{-n}$). As will be shown below, this circumstance opens up the possibility of generating weakly deformed high-peak-power subpicosecond pulses.

Consider the dynamics of FMPs using the example of an initially secant-hyperbolic WP, given by the initial conditions

$$A(\tau, z=0) = A_0\,\mathrm{sech}(\tau/\tau_0)\exp(\mathrm{i}\alpha_0\tau^2), \quad (5)$$

where τ_0 is the initial duration and α_0 is the initial rate of frequency modulation (chirp) of the pulse.

The WP dynamics in an inhomogeneous fibre, taking into account the influence of second- and third-order dispersion effects, is described by the equation [10, 42, 45]:

$$\frac{\partial A}{\partial z} - \mathrm{i}\frac{\beta_2(z)}{2}\frac{\partial^2 A}{\partial\tau^2} + \frac{\beta_3(z)}{6}\frac{\partial^3 A}{\partial\tau^3} + \mathrm{i}R(z)\left(|A|^2 - \tau_R\frac{\partial|A|^2}{\partial\tau}\right)A = 0. \quad (6)$$

Here $\tau = t - \int_0^z \mathrm{d}\xi/u(\xi)$ is the time in the travelling coordinate system; $u(z)$ is the WP group velocity; $R(z)$ is the cubic nonlinearity coefficient; and τ_R is the nonlinear response time of the medium. It was shown in [11–14] that for FMPs with initial conditions (5), within the framework of the approximations $\beta_3(z) \to 0$, $\tau_R \to 0$, and $R(z) = R_0 = \mathrm{const}$, the strong time compression cam be realised in fibres with an exponential second-order GVD distribution profile:

$$\beta_2(z) = -|\beta_{20}|\exp(-2\alpha_0|\beta_{20}|z). \quad (7)$$

In this case, the pulse duration is determined with a good degree of accuracy by the relation [13–15]

$$\tau_s(z) \approx \tau_0\exp(-2\alpha_0|\beta_{20}|z). \quad (8)$$

Thus, the use of fibres with a variable dispersion profile makes it possible to produce high-peak-power USPs.

In the case in question, a sharp decrease in GVD can be achieved by increasing the period Λ of each subsequent grating. As can be seen from relations (2)–(4), this will lead to an increase in the detuning δ and, as a consequence, to a decrease in the corresponding dispersion parameters β_n.

From the point of view of the implementation of optimal time compression of FMPs, the manufacture of long chirped RI gratings (with a length of more than 1 m) with a smooth change in the period and, accordingly, with a smooth change in dispersion parameters is a challenge. In this regard, as dispersing elements with parameters varying along the length, we will consider a sequence of in-fibre gratings with a period Λ_i varying from segment to segment. It is assumed here that only the grating period changes with the fibre length. The average (unperturbed) refractive index n_0 and the modulation depth m in all fibre segments are assumed to be the same.

Figure 2 shows the dependences of the change in the grating period along the fibre length (inset) and the detuning parameter $\delta(z)$ corresponding to the GVD profile approximated by an exponential function. In this case, the width of the spectral interval between the centre wavelength and the centre of the band gap (Bragg wavelength) is estimated as $\Delta\lambda(z) \approx \lambda_0|\omega_0 - \omega_B(z)|/\omega_0 \approx \lambda_0\delta(z)V_g/\omega_0 \approx \lambda_0^2\delta(z)/2\pi n_0$. The dependence of $\Delta\lambda$ on the fibre length is shown in Fig. 3. It can be seen from the figures that as the wave packet propagates in a fibre with inscribed in-fibre gratings, both the detuning parameter δ and the corresponding detunings Δ between the wavelengths significantly increase. This situation

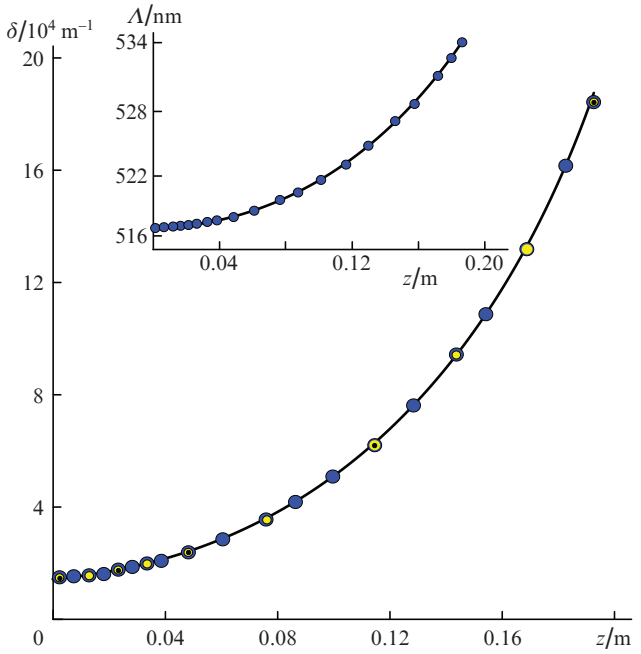

Figure 2. Dependence of the detuning parameter δ on the distance z travelled by the wave packet for a fibre containing (•) 5, (○) 10, and (●) 20 RI gratings. The inset shows the dependence of the period Λ of the RI gratings on the fibre length.

of rapid 'moving away' of the band gap from the centre wavelength of the WP is a feature of the technique proposed in this work.

The main condition for generating high-power FMPs is to provide a rapidly decreasing exponential dispersion profile. In our case, it is achieved by increasing the period of the inscribed RI gratings, which, in turn, leads to an increase in the detuning between the carrier and Bragg frequencies. Therefore, at the fibre exit, the interval $\Delta\lambda$ between the WP centre wavelength and the band gap centre is more than 50 nm with a band gap of about 0.1 nm (see Fig. 3). Thus, the Bragg grating as a dispersing and stabilising element plays a maximum role at the initial stage of pulse propagation. At the final stages of propagation (in the vicinity of the point of maximum compression of the WP), its influence significantly decreases and its linear chirp begins to play the main stabilising role [15, 16].

Figure 4 shows the variation of the second- and third-order dispersion as a function of the length travelled by the pulse in a fibre with a different number of RI gratings. The values for the periods of the gratings were chosen in accordance with the data presented in Fig. 2. The solid line corresponds to a continuous change in the second- and third-order dispersion due to a continuous change in the grating period and detuning parameter, respectively. This situation is realised when a large number (more than 100) gratings with a gradually increasing period are placed along the entire length of the fibre. The dots denote the values of the dispersion parameters of each of the segments of the fibre with sequentially inscribed RI gratings when the fibre is divided into 5, 10, and 20 identical gratings with a length of each element of 4, 2, and 1 cm, respectively.

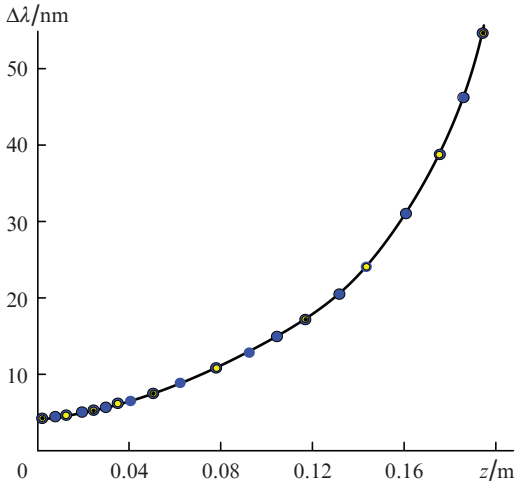

Figure 3. Dependence of the spectral interval between the band gap centre and the centre wavelength of the FMP on the distance z travelled by the wave packet for a fibre containing (•) 5, (○) 10, and (●) 20 RI gratings.

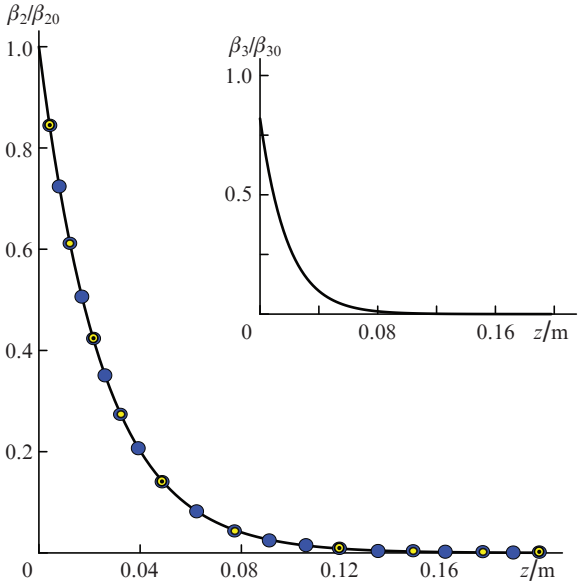

Figure 4. Normalised dependences of the second- and third-order GVD with an exponential profile on the distance z travelled by the wave packet for a fibre containing (•) 5, (○) 10, and (●) 20 RI gratings. The fibre length is 0.19 m, and the dispersion parameters at $z = 0$ are $|\beta_{20}| = 5\times10^{-23}$ s^2 m^{-1}, $|\beta_{30}| = 3.6\times10^{-35}$ s^3 m^{-1}.

3. Compression of FMPs propagating through a fibre with RI gratings. Numerical analysis

Let a pulse with an envelope shape (5), a centre wavelength $\lambda_0 = 1550$ nm, an initial duration $\tau_0 = 10$ ps, a frequency modulation rate $\alpha_0 = 10^{23}$ s^{-2}, and a peak power $P_0 = |A_0|^2 = 7.7$ kW be introduced into a fibre with an unperturbed RI, $n_0 = 1.5$. The Bragg wavelength ($\lambda_B = 2\pi c/\omega_B$) at the fibre input, the detuning, and the grating modulation depth are, respectively, $\lambda_{B1}(z = 0) \equiv 2n_0\Lambda_1 = 1556$ nm, $\delta \approx 2.5\times10^4$ m^{-1}, and $m = 5\times10^{-4}$. The selected parameter values correspond to the coupling coefficient $\kappa \approx 2.5\times10^3$ m^{-1} and the initial parameters of the grating dispersion of the second and third orders: $\beta_2(0) \approx -5\times10^{-23}$ s^2 m^{-1} and $\beta_3(0) \approx 3.6\times10^{-35}$ s^3 m^{-1}. The value of the cubic nonlinearity coefficient $R = 10^{-3}$ (W m)$^{-1}$

is typical for classical single-mode fibres at a wavelength of $\lambda_0 = 1550$ nm for a mode area $S_{\text{eff}} = 50$ μm^2 and a nonlinear response time of the medium $\tau_R \approx 5\times10^{-15}$ s. The dispersion parameters of the second, $d_2 = -2\times10^{-27}$ s^2 m^{-1}, and the third, $d_3 = 10^{-40}$ s^3 m^{-1}, orders are determined by the material of the fibre without the inscribed in-fibre gratings [42, 45]. Note that the influence of the corresponding parameters (especially the parameter d_2) can turn out to be significant at the final stage of pulse compression under conditions when the spectrum width of the wave packet reaches its maximum, and the effect of dispersion parameters due to the presence of in-fibre gratings becomes minimal. As mentioned above, the period of individual gratings was chosen so that the change in GVD could be approximated by some exponential relation of the form $\beta_2(z) = -|\beta_{20}|\exp(-qz)$.

Figure 5 shows the shapes of the FMP envelopes at the output of a fibre containing an RI grating, the change in the period of which provides an exponential second-order GVD profile with $q = 40$ m^{-1}. Since GVD in the fibre in question takes on the values that are orders of magnitude higher than GVD in classical fibre structures, the pulse in such a medium, starting from lengths $z < 0.1$ m, will rapidly compress with simultaneous spectral broadening while maintaining the chirp linearity. For the selected GVD value, the optimal pulse compression is realised at a fibre length $z = 0.19$ m [Fig. 5, curve (*1*)] for a modulation depth $m \approx 5\times10^{-4}$. At large values of m, a subpicosecond pulse with a megawatt peak power is formed over a fibre length of less than 20 cm, while its peak power increases by more than 100 times compared to the initial one. With decreasing m, the relative contribution of third-order dispersion increases, which leads to a decrease in the peak power, an increase in the pedestal, and, as a consequence, to a significant distortion of the pulse envelope. Under certain circumstances, it becomes possible to establish a multi-pulse regime [Fig. 5, curve (*2*)].

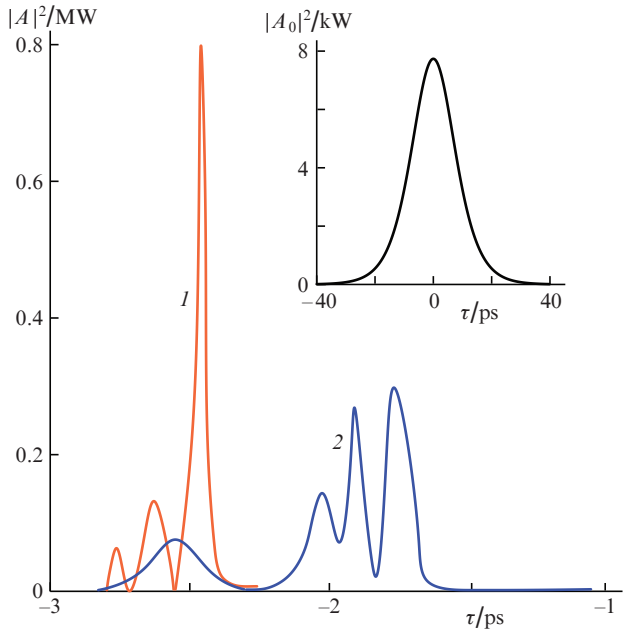

Figure 5. Time profiles of pulses after compression at modulation depths m = (*1*) 5×10^{-4} and (*2*) 10^{-4} and an exponential profile β_2. The inset shows the time profile of the input pulse. The fibre length is 0.19 m.

Note that even when use is made of an RI grating with a small modulation depth, it is possible to generate pulses with peak powers over 100 kW.

In choosing a discrete GVD profile corresponding to a set of gratings with significantly different parameters, the degree and quality of time compression deteriorates. Figure 6 shows the time profiles of the compressed FMP envelope at the output of a fibre containing 5, 10, and 20 RI gratings (the length of each individual grating – except for the last 'shortened' element – is 4, 2, and 1 cm).

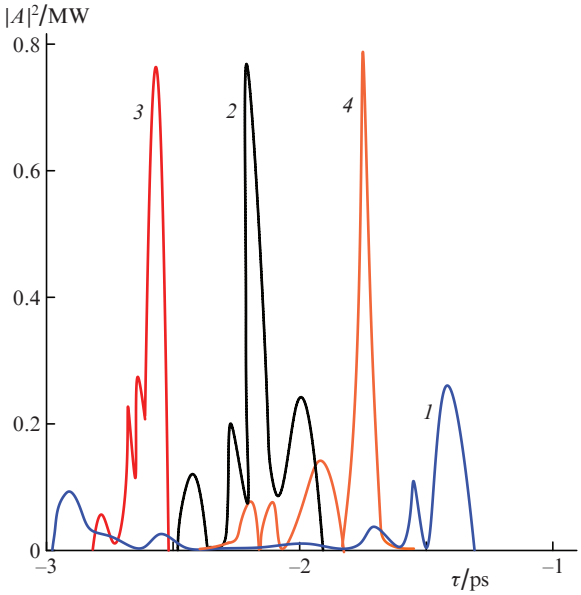

Figure 6. Time profiles of the pulse envelope after compression in a fibre containing (*1*) 5, (*2*) 10, and (*3*) 20 RI gratings, as well as (*4*) in a fibre with a continuous exponential profile β_2 varying along its entire length. The modulation depth is $m = 5\times10^{-4}$, and the fibre length is 0.19 m.

Note that in the case of a sufficiently long fibre having GVD with both a smooth profile and a profile consisting of individual segments, the FMP is rapidly destroyed, and the faster the less smooth the GVD profile. This is clearly seen when comparing the shapes of the pulse envelopes that have passed through a 0.19-m-long fibre. In all cases, the propagation of a pulse through fibres with a periodic segmented or continuous RI profile leads to the appearance of a large number of extraneous noise harmonics on the envelope, despite a very strong increase in the peak power of the main pulse. In this case, the passage through a fibre with a large number of RI gratings provides a higher energy concentration in the main pulse, and the use of a larger number of gratings with shorter periods provides a higher peak power and a smoother pulse pedestal.

4. Conclusions

We have considered the mechanism of compression of picosecond frequency-modulated pulses in fibres with sequentially inscribed refractive-index gratings with stepwise increasing periods (and decreasing GVD). It is shown that such fibres make it is possible to produce subpicosecond FMPS with peak powers of up to 1 MW against the background of a long (relative to the main short pulse) noise pedestal. In the numer-

ical simulation of FMP compression, we have used the values of the parameters of a standard single-mode fibre with an effective mode area $S_{\text{eff}} = 50\ \mu\text{m}^2$ and a cubic nonlinearity coefficient $R = 10^{-3}\ (\text{W m})^{-1}$. For fibres with a large mode area ($S_{\text{eff}} \gg 100\ \mu\text{m}^2$), for example, for gradient quasi-single-mode fibres, the Kerr nonlinearity decreases significantly: $R \ll 10^{-3}\ (\text{W m})^{-1}$. This opens up possibilities for obtaining picosecond pulses with huge (gigawatt and supergigawatt) peak powers using the proposed method.

Separately, we note that, despite the difficulties in fabricating fibres with RI gratings with a total length of more than 1 m, this problem looks quite solvable and very promising. Within the framework of the proposed concept, the use of fibres with a modulation depth of gratings, $m < 10^{-4}$, will ensure the generation of megawatt (and super-megawatt for gradient fibres) peak powers for pulses with an initial peak power of less than 1 kW. The authors intend to return to the consideration of such structures after obtaining the first experimental results demonstrating the efficiency of the above-proposed model.

Acknowledgements. This work was supported by the Ministry of Science and Higher Education of the Russian Federation within the framework of State Task No. 0830-2020-0009, as well as by the Russian Foundation for Basic Research (Project Nos 18-29-1910, 19-42-730005, and 19-42-730013).

References

1. Geddes C.G., Toth C., Tilborg J., Esarey E., Schroeder C.B., Bruhwiler D., Nieter C., Cary J., Leemans W.P. *Nature*, **431**, 538 (2004).
2. Veisz L., Schmid K., Tavella F., Benavides S., et al. *Compt. Rend. Phys*., **10**, 140 (2009).
3. Buck A., Wenz J., Karsch S., Veisz L. *Phys. Rev. Lett*., **110**, 185006 (2013).
4. Caldwell A. et al. *Nature Phys*., **5**, 363 (2009).
5. Bolshakov V.V., Vorob'ev A.A., Uryupina D.S., Ivanov K.A., Morshedian N., Volkov R.V., Savel'ev A.B. *Quantum Electron.*, **39**, 669 (2009) [*Kvantovaya Elektron*., **39**, 669 (2009)].
6. Bahari A., Taranukhin V.D. *Quantum Electron*., **34**, 129 (2004) [*Kvantovaya Elektron*., **34**, 129 (2004)].
7. Lourenco S., Kowarsch N., Scheid W., Wang P.X. *Laser Part Beams*, **28**, 195 (2010).
8. Shank C.V., Fork R.L., Yen R., Stolen R.H., Tomlinson W.J. *Appl. Phys. Lett*., **40**, 761 (1982).
9. Strickland D., Mourou G. *Opt. Commun*., **56**, 219 (1985).
10. Smirnov S., Kobtsev S., Kukarin S. *Opt. Express*, **23**, 3914 (2015).
11. Serkin V.N., Belyaeva T.L. *Pis'ma Zh. Eksp. Teor. Fiz*., **74**, 649 (2001).
12. Serkin V.N., Belyaeva T.L. *Quantum Electron*., **31**, 1007 (2001) [*Kvantovaya Elektron*., **31**, 1007 (2001)].
13. Sysolyatin A.A., Shalygin M.G. *Quantum Electron*., **33**, 265 (2003) [*Kvantovaya Elektron*, **33**, 265 (2003)].
14. Zolotovskii I.O., Korobko D.A., Okhotnikov O.G., Sysolyatin A.A., Fotiadi A.A. *Quantum Electron*., **42**, 828 (2012) [*Kvantovaya Elektron*., **42**, 828 (2012)].
15. Korobko D.A., Okhotnikov O.G., Zolotovskii I.O. *J. Opt. Soc. Am. B*, **30**, 2377 (2013).
16. Korobko D.A., Okhotnikov O.G., Sysolyatin A.A., Yavtushenko M.S., Zolotovskii I.O. *J. Opt. Soc. Am. B*, **30** (3), 582 (2013).
17. Filippov V., Chamorovskii Yu., Kerttula J., Golant K., Pessa M., Okhotnikov O.G. *Opt. Express*, **16**, 1929 (2008).
18. Trikshev A.I., Kurkov A.S., Tsvetkov V.B., Filatova S.A., Kertulla J., Filippov V., Chamorovskiy Yu.K., Okhotnikov O.G. *Laser Phys. Lett*., **10**, 065101 (2013).
19. Andrianov A.V., Koptev M.Yu., Anashkina E.A., Muravyev S.V., Kim A.V., Lipatov D.S., Velmiskin V.V., Levchenko A.E., Bubnov M.M., Likhachev M.E. *Quantum Electron*., **49**, 1093 (2019) [*Kvantovaya Elektron*., **49**, 1093 (2019)].
20. Kuznetsov A.G., Kharenko D.S., Babin S.A. *Quantum Electron.*, **48**, 1105 (2018) [*Kvantovaya Elektron*., **48**, 1105 (2018)].
21. Dong L., Peng X., Li J. *J. Opt. Soc. Am. B*, **24**, 1689 (2007).
22. Koptev M.Yu., Anashkina E.A., Bobkov K.K., et al. *Quantum Electron*., **45**, 443 (2015) [*Kvantovaya Elektron*., **45**, 443 (2015)].
23. Mafi A. *J. Lightwave Technol*., **30**, 2803 (2012).
24. Renninger W.H., Wise F.W. *Nat. Commun*., **4**, 1719 (2013).
25. Krupa K., Tonello A., Barthélémy A., Couderc V., Shalaby B.M., Bendahmane A., Millot G., Wabnitz S. *Phys. Rev. Lett.*, **116**, 183901 (2016).
26. Krupa K., Tonello A., Shalaby B.M., Fabert M., Barthélémy A., Millot G., Wabnitz S., Couderc V. *Nature Photon*., **11**, 237 (2017).
27. Ahsan A.S., Agrawal G.P. *Opt. Lett*., **43**, 3345 (2018).
28. Agrawal G.P. *Opt. Fiber Technol*., **50**, 309 (2019).
29. Conforti M., Arabi C.M., Mussot A., Kudlinski A. *Opt. Lett*., **42**, 4004 (2017).
30. Wright L.G., Ziegler Z.M., Lushnikov P.M., Zhu Z., Eftekhar M.A., Christodoulides D.N., Wise F.W. *IEEE J. Sel. Top. Quantum Electron*., **24**, 5100516 (2018).
31. Wright L.G., Wabnitz S., Christodoulides D.N., Wise F.W. *Phys. Rev. Lett.*, **115**, 223902 (2015).
32. Vasil'ev S.A., Medvedkov O.I., Korolev I.G., Bozhkov A.S., Kurkov A.S., Dianov E.M. *Quantum Electron*., **35**, 1085 (2005) [*Kvantovaya Elektron*., **35**, 1085 (2005)].
33. Kablukov S.I., Zlobin E.A., Skvortsov M.I., Nemov I.N., Wolf A.A., Dostovalov A.V., Babin S.A. *Quantum Electron*., **46**, 1106 (2016) [*Kvantovaya Elektron*., **46**, 1106 (2016)].
34. Zlobina E.A., Kablukov S.I., Wolf A.A., Dostovalov A.V., Babin S.A. *Opt. Lett*., **42**, 9 (2017).
35. Zlobina E.A., Kablukov S.I., Skvortsov M.I., Nemov I.N., Babin S.A. *Laser Phys. Lett*., **13**, 035102 (2016).
36. Wolf A.A., Dostovalov A.V., Vabnits S., Babin S.A. *Quantum Electron*., **48**, 1128 (2018) [*Kvantovaya Elektron*., **48**, 1128 (2018)].
37. Wolf A., Dostovalov A., Bronnikov K., Babin S. *Opt. Express*, **27**, 13978 (2019).
38. Mizunami T., Djambova T.V., Niiho T., Gupta S. *J. Lightwave Technol*., **18**, 230 (2000).
39. Sang X., Yu C., Yan B. *J. Optoelectron. Adv. Mater*., **8**, 1616 (2006).
40. Liu Y., Lit J., Gu X., Wei L. *Opt. Express*, **13**, 8513 (2005).
41. Litchinitser N.M., Eggleton B.J., Patterson D.B. *J. Lightwave Technol.*, **15**, 1303 (1997).
42. Agrawal G. *Nonlinear Fiber Optics* (Berlin: Springer-Verlag, 2007).
43. Eggleton B.J., Slusher R.E., de Sterke C.M., Krug P.A., Sipe J.E. *Phys. Rev. Lett.*, **76**, 1627 (1996).
44. Eggleton B.J., de Sterke C.M., Aceves A.B., Sipe J.E., Strasser T.A., Slusher R.E. *Opt. Commun*., **149**, 267 (1998).
45. Akhmanov S.A., Vysloukh V.A., Chirkin A.S. *Optics of Femtosecond Laser Pulses* (New York: American Institute of Physics, 1992; Moscow: Nauka, 1988).